2011 American Control Conference
on O'Farrell Street, San Francisco, CA, USA
June 29 - July 01, 2011

Constrained Dynamic Control of Focal Trajectory and Intensity of Phased Array Ultrasound Thermal Therapies

Ran Niu and Mikhail Skliar

Abstract— **Long treatment times and normal tissue damage have been identified as major problems of ultrasound (US) surgery when large tumor volumes are treated, or when a tumor is located in close proximity to critical normal tissues. In this paper, a treatment control system that automatically selects location and intensity of the US focal zone to deliver the prescribed thermal dose to the target in minimum time without violating explicitly-imposed normal tissue safety constraints is developed. The controller is characterized by its time-optimal performance and direct incorporation of normal tissue constraints. To minimize the treatment time, which can be substantial with the explicit safety constraints, the control system applies the maximum US power for as long as possible without violating constraints by automatically changing focal zone locations to continue therapy at the maximum possible power. When there are no untreated locations where the maximum power can be applied without violating safety objectives, the control system selects focal locations and intensities such that the treatment is completed with at least one of the safety constraints active. The developed approach is evaluated in a computer-simulated treatment of a patient-specific three-dimensional breast tumor heated by an US phased array system.**

I. Introduction

Noninvasive or minimally invasive thermal treatments use energy of ultrasound or electromagnetic sources to selectively heat the target tissue to a lethal or sub-lethal dose. Lethal heating causes tissue necrosis and coagulation, while sublethal treatments are used as an adjuvant to other therapies, or during thermally activated targeted drug delivery. The efficacy of moderate and high temperature thermal therapies has been demonstrated in a number of clinical trials for different anatomical sites [5]. Moderate temperature hyperthermia causes numerous biological effects and is an effective adjuvant anti-cancer treatment modality to chemo- and radiation therapies [4].Thermal ablation or high temperature thermal therapies can be used as an effective stand-alone thermal surgical procedure to generate tissue necrosis and cellular coagulation.The clinical ablation of benign breast fibroadenomas [8], localized prostate cancer [13], uterine leiomyomas [9] using high-intensity focused ultrasound (HIFU) have been reported.

Long treatment times, incomplete treatment of large targets, and unintended normal tissue damage continue to impede a broader penetration of HIFU therapies into clinical practice. These problems may be traced back to the adopted methods to achieve treatment efficacy and the lack of explicit specification of normal tissue safety as one of the objectives of the of the automatic treatment control systems. For example, to avoid over-heating of surrounding critical normal tissue while heating the tumor, sufficient cooling periods are introduced between usually multiple sonications [10]. A small focal region of focused ultrasound transducers requires a large number of ultrasound pulses placed in different tumor locations to cover the entire treatment volume, each separated by cooling intervals, which are typically 90 s long. The result is a very long total treatment time [7] for large tumors. Treatment of the tumors in proximity of important normal tissues further increases the treatment time because of the typical conservative approach of lowering the applied power and increasing cooling intervals between consecutive pulses.

Our approach to address existing limitations is characterized by direct control of the thermal dose (TD) in HIFU therapies while simultaneously requiring the control system to satisfy the explicit safety constraints, imposed in the form of the maximum allowed temperatures in selected normal tissue locations. Explicit incorporation of competing safety and efficacy objectives into the operation of the treatment control system may lead to long treatments. Therefore, we emphasize the need to balance safety and efficacy in the minimum treatment time. In the case of a single focused ultrasound transducer with a fixed focal zone, the proposed approach was previously tested in phantoms and *in-vivo* [2], including the case of real-time MR-thermometry feedback [1].

In this paper, we describe a treatment control system, which automatically controls both the location of the focal zone and the ultrasound intensity of an ultrasound phased array in order to safely and rapidly deliver the prescribed TD to the tumor without violating the imposed normal tissue safety constraints. The automatically selected focal locations are such that the target is treated with the maximum possible ultrasound intensity while satisfying the imposed normal tissue constraints in the surrounding normal tissue to ensure safety. Performance and robustness of the proposed treatment control system was tested in a simulated ultrasound phased array treatment of a patient specific tumor. The results demonstrate that the developed dynamic controller successfully delivers the prescribed TD to the target in the minimized treatment time while satisfying safety constraints.

II. Methods

A. Problem Statement

Deliver the physician-prescribed thermal dose, $D_f(r)$, to the entire three-dimensional treatment target in the minimum time by automatically selecting the location and intensity of ultrasound focal zone. Achieve the above efficacy objective

R. Niu was with the Univ. of Utah, now with Real-time Controls & Instrumentation Laboratory at GE Global Research, Shanghai, 201203, China.

M. Skliar is with University of Utah, Salt Lake City, UT 84112, USA (corresponding author, e-mail: mikhail.skliar at utah.edu)

without violating the maximum allowable temperatures in the normal tissues surrounding the target.

B. Thermal and Acoustic Models

1) Thermal Dose Model: Thermal dose defined as cumulative equivalent minutes (CEM) at 43°C , introduced by Sapareto and Dewey [15], is broadly used to quantify efficacy of thermal therapies. Assuming an Arrhenius relationship between temperature and the dose, the time interval $\triangle t$ during which the tissue was maintained at temperature T is converted into an equivalent (from the perspective of the delivered thermal dose) time at the standard temperature $T_{eq} = 43°\text{C}$:

$$\Delta t_{eq} = \Delta t R^{(T_{eq}-T)}, \tag{1}$$

where empirical constant $R = 0.5$ for $T \geq 43°$ C, $R = 0.25$ for $43° > T \geq 39°$ C and $R = 0$ for $T < 39°$ C [16]. For a continuously changing T, the TD is therefore defined as:

$$D(r,t) = \text{CEM at } 43°\text{C} = \int_0^t R^{[43-T(r,\tau)]} d\tau \tag{2}$$

2) Thermal Treatment Models: Thermal transport in tissues is often described by the Pennes' bioheat transfer equation (BHTE) [12]:

$$\rho C \frac{\partial T(r,t)}{\partial t} = \nabla \cdot (k \nabla T(r,t)) - W_b C_b T(r,t) + Q(r,t) \tag{3}$$

where T (°C) is the tissue temperature, C and C_b are the specific heat of tissue and blood (J/kg/°C), and W_b (kg/m^3/s) is the blood perfusion related parameter; ρ (kg/m^3) and k (W/m/°C) are the tissue density and thermal conductivity, and T_a is the arterial or baseline temperature. Q (W/m^3) described the power deposited in the tissue. The full and reduced order approximations of the heat transfer model in the state space form are expressed as:

$$\begin{aligned} x(k+1) &= Ax(k) + Bu(k) \\ T_m(k) &= Cx(k) \end{aligned} \tag{4}$$

where $x(k) \in R^n$ is the state vector, matrix A characterizes tissue cooling to the equilibrium by heat conduction and convection. Focused US heating is described by the term $Bu(k)$ which describes the specific absorption rate (SAR) of the US energy for a given focal position inside the tumor. The input vector $u(k)$ describes the intensity (in Watts) of the applied ultrasound, while B characterizes spatial distribution of the applied energy as a function of the focal zone location. If we assume that the treatment is monitored in every spatial location by magnetic resonance thermometry, $T_m(k) \in R^m$ is the measured temperature in each voxel within the target and the surrounding normal tissue.

3) Beam Propagation Model: The ultrasound beam propagation was simulated for a custom designed MRI compatible ultrasound phased array transducer used in the experiments. The transducer, shown in Figure 1, consists of 256 elements, randomly arranged on a curved surface to reduce side lobes. The intensity and phasing of each element can be controlled independently, which allows for an electronic steering of the focal zone within the target.

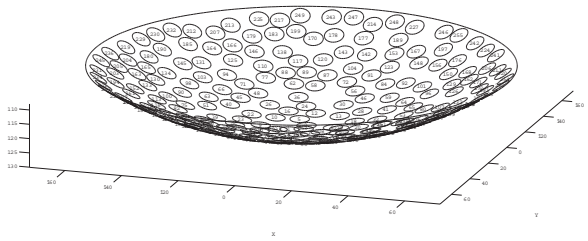

Fig. 1. 256-element MRI compatible US phased array transducer system.

To model the beam propagation in the inhomogeneous tissue we used an extension of the traditional angular spectrum method - hybrid angular spectrum (HAS) method [18]. This method is a spatial-frequency domain technique in which an arbitrary spatial pattern is encoded into a spectrum of plane waves, each traveling at a unique angle. Using fast Fourier transform (FFT), the technique transforms an input pressure pattern into a collection of propagating waves in the frequency domain and propagates these plane waves using a linear propagation filter. The plane waves are then transformed back into the space domain using the inverse fast Fourier transform (IFFT) to obtain the pressure pattern in space. In the hybrid angular spectrum technique, the inhomogeneous tissue model is broken into voxels, each voxel having a unique speed of sound, absorption coefficient and density. Each plane of voxels is collapsed into an equivalent thin layer with varying acoustic properties in x and y directions.

To find the pressure pattern at distance z from the input pressure pattern, the calculations alternate between the space domain and the frequency domain for each layer, resulting in a computationally efficient approach.

C. Thermal Dose Controller

1) Control Structure: The developed treatment control system was designed to manipulate the focal position and the corresponding ultrasound intensity in order to automatically deliver in minimum time the prescribed thermal dose, $D_f(r)$, $r \equiv (x,y,z)$, to the tumor (in CEM) without violating normal tissue safety constraints. The safety constraints, in the form of the maximum allowable normal tissue temperature, were imposed on an ellipsoidal surface enclosing the tumor. The maximum power of the ultrasound array was constrained to reflect hardware limitations and to prevent tissue cavitation. The system was designed assuming that the temperature feedback is provided by MR-thermometry.

A simplified structure of the developed control system is depicted in Figure 2. The temperature distribution $T_m(r,k)$, measured by MR thermometry, was used to estimate the thermal dose $D_m(r,k)$ (block H_m) delivered up to the current treatment time, k. Temperatures distribution, $T_m(r,k)$, was also used in a Kalman filter, used to estimate states $x(k)$. The estimated states, measurements $T_m(r,k)$, and the dose deficit, $D_f(r) - D_m(r,k)$ were used as an input to the treatment controller, K_D, which selected the next focal zone location, $p(r,k)$, and corresponding US intensity, $u(k)$.

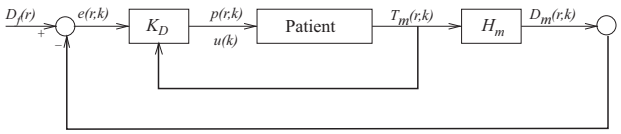

Fig. 2. Simplified block diagram of the HIFU treatment controller.

2) Calculation of $p(r,k)$ and $u(k)$.: Explicit incorporation of safety constraints into the design of the HIFU control system has the potential to significantly increase the treatment time in order to balance safety and efficacy objectives. This makes the problem of minimizing the treatment time especially important in our approach.

Pontryagin's maximum principle [14], applied to the problem of the constraint minimum-time delivery of the thermal dose, gives an important necessary condition for time-optimality of HIFU treatments: At least one of the inequality constraints – on maximum allowed normal tissue temperature in one or more locations and/or the ultrasound intensity, $0 \leq u(k) \leq I_{max}$ – must be active throughout the treatment. The necessary conditions of time optimality alone are not sufficient for the design of the minimum-time treatment control system because they are satisfied by infinitely many solutions, corresponding to different combinations of inequality constraints active at different times during the treatment. Therefore, additional conditions must be added to arrive at a unique treatment strategy.

To derive such conditions, consider the treatment time, t_f, which we wish to minimize by selecting the focal trajectory, $p(r,k)$, and the corresponding ultrasound intensity, $u(k)$. Note that for the minimum-time treatments, $t_f \leq t_I + t_T$, where t_T is the cumulative time the treatment progressed with active normal tissue temperature constraints and $t_I = t_0 + t_{I_{max}}$ is the cumulative time the ultrasound intensity was either at the maximum ($t_{I_{max}}$) or zero level. The above relationship between t_f, t_I, and t_T becomes an equality if during the minimum-time treatment the ultrasound power and safety constraints are never active simultaneously. Therefore, $p(r,k)$ and $u(k)$ which minimize the treatment time solve the following minimax problem:

$$\min_{p,I} \max_{t_{I_{max}}} (t_{I_{max}} + t_0 + t_T) \tag{5}$$

By posing the treatment minimization as a minimax problem (5) allows us to establish the following conditions (partial list), which were used in the implementation of the developed HIFU control system:

1) Condition for changing focal location:
   a) The controller must select a new location if the TD has reached its target value in the current location.
   b) If the treatment in the current location requires that the controller lowers the ultrasound intensity to avoid the violation of safety constraints, the selection of the focal position must re-evaluated by the controller using the available treatment models.
2) Selection of a new location & the corresponding power:
   a) The controller uses the SAR (ultrasound absorption) and thermal response models of the patient to determine focal positions where the power can be kept at the maximum values without violating safety constraints.
   b) If more than one such position exists, the controller moves the focal zone into the location with the highest temperature to take advantage of the highly nonlinear temperature-thermal dose relationship.
   c) Additional conditions were established for treating tumor edges and when there are no possible focal locations such that the treatment can proceed with maximum ultrasound power.

Alternative conditions were also evaluated and are not reported here. In the current implementation, the controller makes the selection of a new focal zone based on model prediction over a limited time horizon, which limits the capability to account for future heating due to the overlap in the ultrasound beam patterns focused on different locations.

3) Dose Controller - K_D: The designed control system continuously treats the target at the maximum possible power for as long as possible by changing focal positions as necessary to avoid normal tissue constraint violation. Model predictions are used to determine focal locations where the maximum power can be applied and, when multiple choices exist, the position with the highest current temperature is selected. Predetermined cooling intervals are not used.

In all but the simplest cases of small tumors that are not in the proximity of critical normal tissues, the treatment at the maximum power cannot proceed to completion. Typically, thermal build-up in and around the target, partial heating of the intervening normal tissue, and heat conduction and convection from the target are all combined to elevate normal tissue temperatures to the point when treatment can no longer proceed at the maximum applied power without violating normal tissue constraints.

The maximum possible power, $u(c_i,k)$, that will not lead to the violation of the normal tissue constraints T_{max} in the location $r = c_i$ can be calculated from the model as

$$T_{max} = \hat{y}(c_i, k+1) = (CA)_{i,j}\hat{x}_{k|k} + (CB)_{i,j}u(c_i,k) \tag{6}$$

where $\hat{y}(c_i, k+1)$ is the estimated temperature in c_i at the next sampling time. To accelerate the calculations, the determination of u is based on the reduced order model, the estimated state vector of which, $\hat{x}_{k|k}$, is obtained using the Kalman filter. For a given constraint location c_i the calculation of u should be repeated for all possible focal zone locations. The end result is the maximum possible power and the corresponding focal zone location that does not lead to the violation of the normal tissue constraint in the location c_i. The process is then repeated for all constrained locations, and the next focal position is selected as the one where the maximum power can be applied without violating any of the imposed normal tissue constraints.

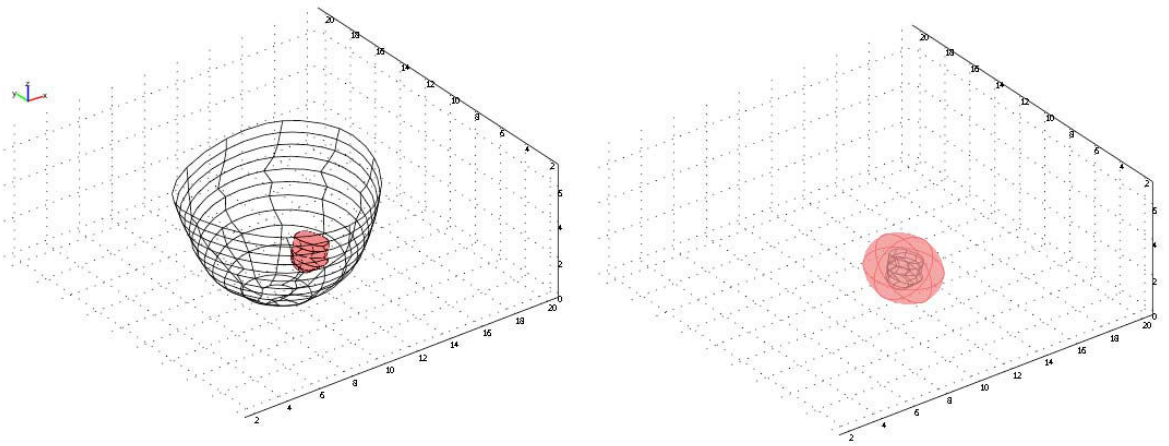

Fig. 3. a) Breast & tumor geometries. b) Normal tissue temperature constraints were imposed in 209 locations on ellipsoidal surface containing the tumor.

III. Results

A. Patient Model

The patient has bilateral breast cancer with a primary invasive tumor in the anterior periareolar region of the left breast. A threshold segmentation algorithm was used to segment the dynamic contrast enhanced (DCE) MRI data into the tumor, fibroglandular tissue, fat and background air. The primary invasive tumor close to the skin on the left breast was selected as the thermal therapy target. The geometry of the breast and the tumor was obtained by automatic segmentation of 104 contrast-enhanced MRI coronal images with $1.5\times1.5\times1.5$ mm spatial resolution. It was assumed that normal tissue outside the primary tumor has the properties of the normal fat tissue.

Figure 3(a) shows the geometry of the obtained breast and tumor model. The breast is almost hemispheric while the tumor has very irregular shape. The tumor is 1.5cm away from the skin and more than 3.6cm away from the rib cage in the z axis. Figure 3(b) shows an ellipsoidal surface of constrained normal tissue locations. This surface encloses the tumor and is at least 0.9cm away from its boundary. Due to the irregular shape of the tumor, in most cases, the distance between the tumor and constrained surfaces is approximately 1cm. The total number of constrained normal tissue locations on the ellipsoidal surface was 209.

The detailed finite element (FE) model of the thermal response of the breast tumor to ultrasound heating, consisting of $15,911$ tetrahedral elements, was used to model the patient. The bioheat transfer model was used to describe the temperature response to the applied ultrasound. The deposited energy Q was obtained from the modeling of the ultrasound beam propagation. See Table I for the thermal and acoustic properties used in the simulation. A breast surface temperature was assumed to be maintained at 37°C. An initial temperature prior to sonication was 37°C. FEM solver (COMSOL) was used to calculate the temperature response to the sonication. The FE model had $22,674$ degrees of freedom. To obtain the model used in the treatment control system, a coarse FE model with 13523 degree of freedom and 9299 tetrahedral elements was obtained first. This model was then converted into the state space form and the balanced model reduction [17] was then used. The reduced order model has 1143 states, and 209 outputs equal to the number of the constrained normal tissue locations. The monitoring of the treatment progression and the calculation of the delivered dose was done assuming that MR thermometry measurements are available for the entire tumor.

TABLE I

Thermal and acoustic properties used in simulation [6], [11]

	k W/(m°C)	ρ kg/m^3	$C=C_b$ J/(kg°C)	W kg/m^{3}s	c m/s	α 1/cm/MHz
Fat	0.5	937	3550	0.5	1480	0.086
Tumor	0.5	1064	3770	1	1560	0.133
Blood	0.5	1000	4000	1	-	-
Water	-	1000	-	-	1500	0

B. Phased Array Simulation

Hybrid angular spectrum method was used to simulate the 256-element ultrasound phased array system, fabricated with the support of Siemens Medical Solutions. This array operates at 1MHz, with aperture diameter of 13cm, equal to the radius of the curvature on which the array elements were randomly positioned. In simulations, the array was located 11cm away from the breast surface and in an orientation such that the axis of the focal beam coincided with the z-axis in Figure 3. The transducer was assumed to be placed in a bath of water, providing acoustical coupling to the patient. The acoustic properties used in the simulation are given in Table I [3], where c is the speed of sound (m/s) and α is the attenuation coefficient (1/cm/MHz).

Figure 4 gives an example of the power deposition patterns, Q, created inside the tumor by the described array. In this example, the focal zone is located at the center of the tumor at $(x,y,z)=(10.95,8.7,2.4)$cm. The total acoustic

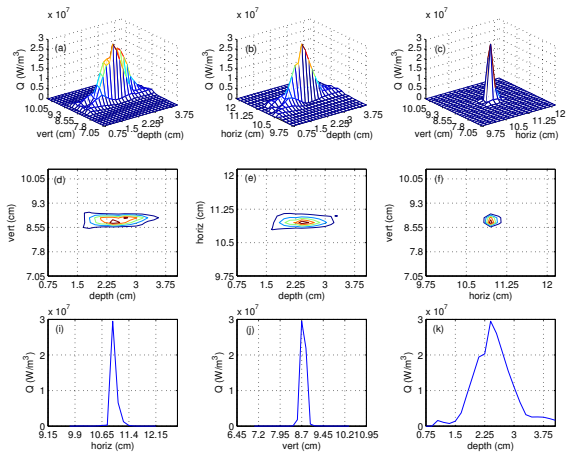

Fig. 4. (Top) Power deposition pattern through tumor center on (a-b) axial planes (c) focal plane. (Middle) Power deposition contour on (d-e) axial planes and (f) focal plane. (Bottom) Power deposition along (g) horizontal, (h) vertical and (i) depth direction respectively.

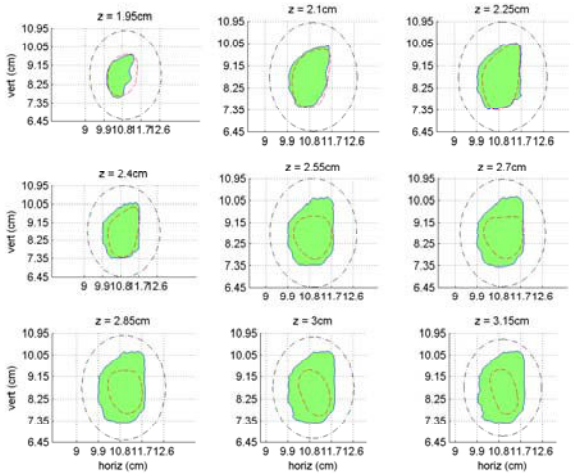

Fig. 6. Thermal lesion created at the end of the treatment on each coronal image, (dashed dotted line) constrained ellipsoidal surface, (dashed line) irregular tumor boundary.

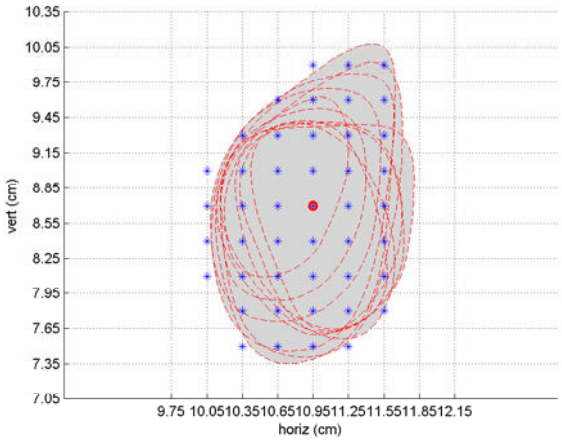

Fig. 5. Treatment planning, dashed lines are the tumor boundaries of each coronal image, $*$ denotes the pre-selected focal zone locations on the focal plane of $z = 2.4$cm, $\circ$ denotes the tumor center.

power radiated from transducer face is 22W. Figure 4 (a-c) correspond to the power deposition pattern through the tumor center on two axial planes and the focal plane through the focal zone, (d-f) show the power deposition contour, and (h-j) show the power deposition along the horizontal, vertical and depth directions, respectively.

C. Treatment Planning

A tumor volume is usually sonicated by dividing it into one or more planes perpendicular to the beam propagation direction, in which focal zones may be placed. The locations of the focal zones in both radial and axial directions must be dense enough to ensure the complete treatment of the entire volume. The focal zone placement is highly dependent on the characteristics of a transducer used during therapy.

For the case of our phased array transducer and the specific tumor considered in this paper, a single focal plane was selected. This plane was normal to the z axis and crossed the tumor in its approximate center located at $z = 2.4$cm. The spacing of the focal zones in that plane 3mm, which provides sufficient focal zone overlap to ensure the complete treatment of the targeted volume. The focal zones were restricted to 45 locations, depicted in Figure 5. The numbering of the foci is on the raster pattern, increasing in the horizontal direction for each fixed vertical position. Figure 5 also displays the tumor boundary for each coronal image used to reconstruct the tumor geometry. The maximum ultrasound power was constrained to $I_{max} = 22$W for all focal locations to avoid excessive temperatures to prevent boiling and gas formation.

D. Treatment Results

The treatment control system was required to deliver a thermal dose of at least 240 CEM at 43° T_{90} to the entire tumor without violating the normal tissue constraints of 6 °C above the 37°C. A total of normal tissue constraints were imposed in 209 locations evenly distributed on the ellipsoidal surface shown in Figure 3(b). It was assumed that the MR-thermometry provided temperature measurements every 2s.

Fig. 6 shows the thermal lesion (green) where at least 240 CEM of the thermal dose was delivered. For different values of z, the ellipsoids (dashed lines) show the cross-sections of the surface on which normal tissue constraints were imposed. Tumor boundary is shown as an irregular dashed red line. Except for the z locations below 2.1cm, the tumor region was completely treated. The incompletely treated volume is the closest to the array and the skin surface, which was maintained at 37°C in the water bath. Retrospective analysis indicates that the treatment would improve if an additional focal plane is introduced closer to the transducer.

Fig. 7(a)-(b) shows the controller-selected US power and the corresponding transducer focal zone locations for the first 500s of the treatment. Fig 7 (c) shows the temperature evolution in selected constrained normal tissue locations where

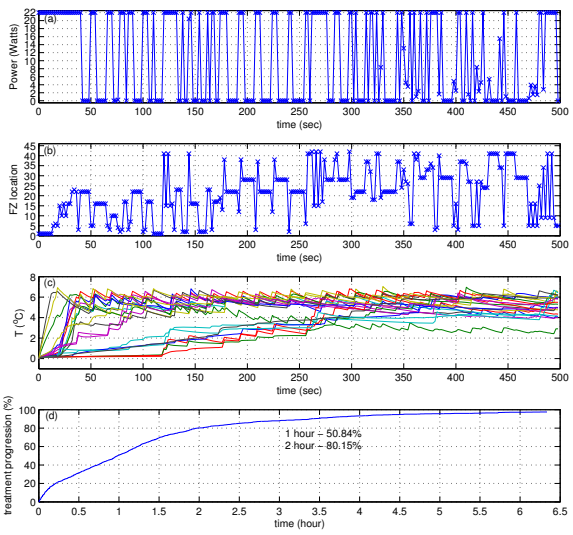

Fig. 7. (a)-(b) Controller selected transducer power and corresponding focal zone locations for the first 500s of the treatment. (c) Temperature evolution in selected constrained normal tissue locations for the first 500s. (d) Treatment progression as a function of time.

the maximum allowable temperature of 6 °C was occasionally violated. These violations are caused by modeling errors, and relatively slow sampling of the MRI thermometry.

Fig. 7(a) shows that initially, the control system applied the maximum power. The focal zone (FZ) was maintained at the initial location 1 (the bottom left focal position in Figure 5) for about 12sec, after which one of the constraints was violated. The controller selected new FZ positions that allowed it to maintain the maximum power for ∼40 s. After that, based on the available thermal and SAR models, the controller was not able to find any focal position that did not lead to the normal constrained violation, so the power was switched off. The next selection of the FZ and the corresponding power was evaluated 2s later, after new temperature measurements became available. After all constrained temperatures cooled below the set limit, a new location was chosen.

After the initial 40s, the US power was modulated between $I = 0$ and $I = I_{max}$. Rapid power modulation is an expected behavior of the constrained minimum-time control system. Also note that the treatment progresses close to the normal tissue constraints, as one would expect during the minimum-time treatment without cooling intervals.

Fig. 7(d) shows percent tumor treated as a function of time. Initially, the treatment progression towards the efficacy objective is fast, but slows considerably after thermal buildup and consistent activation of normal tissue constraints.

IV. Conclusion and Discussion

This paper presents the development and evaluation of a minimum-time constrained trajectory control of thermal treatment. The developed controller delivers the prescribed thermal dose to the tumor safely and accurately. This is achieved by automatic real-time manipulation of the focal trajectory and the corresponding ultrasound intensity.

The performance of the developed control system was evaluated in computer-simulated US ablation of patient specific breast tumor sonicated by 256-element phased array. The results demonstrate the feasibility of the explicit control of efficacy and safety in HIFU therapies by automatic manipulation of focal trajectory and intensity of an US phased array, and clearly indicated the need to further investigate control strategies that minimize the overall treatment time.

V. Acknowledgments

Funded by NIH (NCI-R01-CA33922), NSF (CTS 0117300), and Siemens Medical Solutions. Dr. M. Schabel provided MRI images of the breast patient. Beam propagation model was provided by Dr. D. Christensen and Ms. U. Vyas.

References

[1] D. Arora, D. Cooley, T. Perry, J. Guo, A. Richardson, J. Moellmer, R. Hadley, D. Parker, M. Skliar, and R. B. Roemer, "In-vivo evaluation of a MR thermometry based thermal dose control system for focused ultrasound thermal treatments," *Int. J. Hyperthermia*, vol. 22, pp. 29–42, 2006.

[2] D. Arora, D. Cooley, T. Perry, M. Skliar, and R. Roemer, "Direct thermal dose control of constrained focused ultrasound treatments: Phantom and *In-Vivo* evaluation," *Physics in Medicine and Biology*, vol. 50, pp. 1919–1935, 2005.

[3] D. Christensen, *Ultrasonic Bioinstrumentation*. New York: John Wiley & Sons, 1988.

[4] M. Dewhirst and P. Sneed, "Those in gene therapy should pay closer attention to lessons from hyperthermia," *Int. J. Radiat. Oncol. Biol. Phys.*, vol. 57, pp. 597–599, 2003.

[5] C. Diederich, "Thermal ablation and high-temperature thermal therapy: Overview of technology and clinical implementation," *Int. J. Hyperthermia*, vol. 21, pp. 745–753, 2005.

[6] F. A. Duck, *Physical properties of tissue: a comprehensive reference book*. London: Academic, 1990.

[7] X. Fan and K. Hynynen, "Ultrasound surgery using multiple sonifications-treatment time considerations," *Ultrasoind in Med. and Biol.*, vol. 22, pp. 471–482, 1996.

[8] K. Hynynen *et al.*, "MR imaging-guided focused ultrasound surgery of fibroadenomas in the breast: A feasibility study," *Radiology*, vol. 219, pp. 176–185, 2001.

[9] N. McDannold *et al.*, "Uterine leiomyomas: MR imagingc based thermometry and thermal dosimetry during focused ultrasound thermal ablation," *Radiology*, vol. 240, pp. 263–272, 2006.

[10] N. McDannold and F. Jolesz, "Magnetic resonance image guided thermal ablation," *Topics in Magnetic Resonance Imaging*, vol. 11, pp. 191–202, 2000.

[11] M.Malinen, T.Huttunen, K.Hynynen, and J.P.Kaipio, "Simulation study for thermal dose optimization in ultrasound surgery of the breast," *Med. Phys.*, vol. 31, pp. 1296–1307, 2004.

[12] H. Pennes, "Analysis of tissue and arterial blood temperatures in resting human forearm," *J. Appl. Physiol.*, vol. 1, pp. 93–122, 1948.

[13] L. Poissonnier *et al.*, "Results of transrectal focused ultrasound for the treatment of localized prostate cancer," *Prog. Urol.*, vol. 13, pp. 60–72, 2003.

[14] L. Pontryagin *et al.*, *The Mathematical Theory of Optimal Processes*. New York: Wiley, 1962.

[15] S.A.Sapareto and W.C.Dewey, "Thermal dose determination in cancer therapy," *Int. J. Oncol. Biol. Phys.*, vol. 10, pp. 787–800, 1984.

[16] D. Thrall *et al.*, "Using units of CEM 43°C T_{90}, local hyperthermia thermal dose can be delivered as prescribed," *Int. J. Hyperthermia*, vol. 16, 2000.

[17] A. Varga, "Model reduction software in the SLICOT library," *Applied and Computational Control, Signals, and Circuits, Ed. B. Datta*, vol. 2, pp. 239–282, 2001.

[18] U. Vyas and D. Christensen, "Hybrid angular spectrum method for ultrasound beam propagation," in *3rd Annual Mountain West Biomedical Engineering Conference*, 2007.